

# A Low-Cost LED-Based Solar Simulator

Eduardo López-Fraguas<sup>1</sup>, José M. Sánchez-Pena<sup>1</sup>, *Senior Member, IEEE*, and Ricardo Vergaz<sup>1</sup>

**Abstract**—Solar simulators are a fundamental instrument to characterize solar cells parameters, as they can reproduce the operating conditions under which the solar cells are going to work. However, these systems are frequently big, heavy, and expensive, and a small solar simulator could be a good contribution to test small prototyping devices manufactured in research labs, especially if it could manage the irradiation at any wavelength interval in a custom way. We have designed, developed, and calibrated a small solar simulator made entirely with LEDs, no optics inside, and electronically controlled through a PC using an Arduino microcontroller. The whole structure is 3-D printed in black PLA plastic. The electrical current through the LEDs, and thus the spectral irradiance of the simulator, is controlled with a very intuitive LabVIEW interface. As our calibration proves, we have built an easily reproducible and low-cost Class AAA solar simulator in a central illumination area of 1 cm<sup>2</sup>, according to the IEC60904-9 standard. This means that the homogeneity in that area is under a 2% deviation in spatial terms, below 0.5% in temporal terms, and is a factor of a 3% close to the AM1.5G sun reference spectrum. The system can be built and used in any research lab to get quick tests of new small solar cells of any material.

**Index Terms**—AM15G, LED technology, solar cells, solar simulator, ultralow cost.

## I. INTRODUCTION

GREEN energy is a must for the future of our planet. The sun is the best natural available energy source that we have. Photovoltaics (PVs) market of thin-film solar cells was valued at \$11 421 million in 2016 and is projected to grow at a compound annual growth rate of 19.4% from 2017 to 2023, to reach \$39 512 million by 2023, according to PV Market Alliance. The research on new solar cells is currently focused on multijunction, organic, and perovskite solar cells. One of the main processes to be performed in this paper is the optical and electrical responses of the prototype cells to the light as well as their degradation processes.

Solar simulators are used to illuminate the cells during the measurement of their properties to obtain  $I$ - $V$  curves, external quantum efficiency, or electrochemical impedance

spectroscopy (EIS). Solar simulators must accomplish the sun spectrum standards set by the International Electrotechnical Commission (IEC) or American Society for Testing and Materials [1], such as the so-called AM1.5G, which is the global irradiance that reaches the earth surface at an air mass of 1.5 around 100 mW/cm<sup>2</sup>. Light emerging from the light sources in a sun simulator must be controlled in spectral content (typically using filters), temporal stability (typically using complex power sources), and irradiance spatial uniformity (typically using auxiliary optics). Each one of these items provides the sun simulator with a different Class. Class A simulators must match the sun standard in a factor of 0.75–1.25 in each spectral interval. If the factor range widens from 0.6 to 1.4 they are Class B and Class C if the factor ranges from 0.4 to 2. Regarding spatial homogeneity, Class A stands for values below 2%, Class B for 5%, and Class C for 10%. In terms of temporal instability, a deviation factor below 0.5% is allowed for Class A, 2% for Class B, and 5% for Class C. Therefore, the Class AAA simulator reaches the A for the three items.

Solar simulators have been traditionally manufactured using xenon short-arc lamps or metal halide discharge lamps [2] using optical and complex structures [3], [4], for testing special operation environment [5], thermal collectors [6], or even spectroradiometers [7]. However, they need to be warmed up and cooled down, need a hard maintenance and have a quite limited under-specifications lifetime. High-power LED technologies have boosted in the past years in a wide range of spectral intervals due to their use in multiple applications in the market. Thus, LED-based solar simulators have been created to substitute xenon ones in the past decade. They are also able to irradiate in a wide spectral range, especially since the blue LED input in the market [8]. While giving similar results when used to characterize solar cells, they offer a number of advantages over the halogen lamps such as [9]: precision control of their emission both in temporal and intensity terms via software, fast switching and configurable modes, high-power efficiency, tunable spectral distribution using different ranges for exploring different physical and chemical effects at the absorption layers in the cells, more environmentally friendly because no mercury or heavy metals are present, and long life. LEDs simulators are being used both in inorganic [10] and organic PVs generic characterization [11], [12]. Their most promising applications are expected to take the advantage of the ability to tune the spectral emission, which can make different effects in the solar cells operation arise, depending on the energy of the incident photons [13]. They can also be used to drive specific characterizations, from external quantum efficiency fast retrieval [14] to study dew formation in outdoor conditions [15]. Of course, LED illumination is interesting

Manuscript received December 12, 2018; accepted February 4, 2019. Date of publication March 5, 2019; date of current version November 8, 2019. This work was supported in part by the Spanish Ministerio de Economía y Competitividad through AEI/FEDER, UE Funds under Grant TEC2016-77242-C3-1-R and in part by the Comunidad de Madrid SINFOTON-CM Research Program under Grant S2013/MIT-2790. The work of E. López-Fraguas was supported by the Ministerio de Educación y Formación Profesional for his Doctoral Grant through FPU Research Fellowship under Grant FPU17/00612. The Associate Editor coordinating the review process was Emanuele Zappa. (Corresponding author: Eduardo López-Fraguas.)

The authors are with the Displays and Photonics Application Group, Universidad Carlos III de Madrid, 28911 Leganés, Spain (e-mail: edlopezf@ing.uc3m.es; jmpena@ing.uc3m.es; rvergaz@ing.uc3m.es).

Color versions of one or more of the figures in this article are available online at <http://ieeexplore.ieee.org>.

Digital Object Identifier 10.1109/TIM.2019.2899513

for light harvesting also by itself, due to its widespread use in luminaries [16].

Some attempts have been made to create customized, low-cost, and wide spectral range LED simulators like the one presented in this paper. Among them, the work by Krebs *et al.* [17] is remarkable. It tried to mimic the AM1.5G sun spectrum using 18 different wavelengths from 390 to 940 nm, illuminating a  $3.6 \times 2.6 \text{ cm}^2$  aperture and using gas flow to control the atmosphere of the experiment. The layout comprises a dense  $47 \times 17 \text{ mm}^2$  package in lines of seven LEDs, up to a total of 182 LEDs, thus requiring cooling. Digital-to-analog converters (DACs) are used as voltage-to-current drivers to assess the current through the LEDs. Grandi *et al.* [18] combined a 115 € set formed by a halogen lamp and six types of LEDs to get a Class B simulator in a  $10 \times 10 \text{ cm}^2$  area. Stuckelberger *et al.* [19] improved the performance to a 4 suns AAA simulator between 400 and 750 nm in an  $18 \times 18 \text{ cm}^2$  area, using a current control feedback loop and off-the-shelf LEDs, with a notorious cooling structure, and using mirrors to control the light path. However, in this case, the 4 suns are achieved using an equivalent value specifically defined to match with the obtained spectral range. Plyta [20] introduces the novelty of applying an algorithm to select the best possible LEDs to achieve a 24 wavelengths–624 LEDs sun simulator for a  $32 \times 32 \text{ cm}^2$  area as well as a MATLAB program to compute the optimum distribution of the LEDs. Novičkovas *et al.* [21] use only 19 high-power LEDs to illuminate a  $6 \times 6 \text{ cm}^2$  area, ranking a Class A simulator. Such a low number of LEDs was achieved by selectively using secondary optics for several LED groups and taking the advantage of the wide emission angle for others.

A lot of companies have developed commercial LED-based sun simulators following these initial experimental attempts, ranging from wide areas and thousands of LEDs (Glenn-LED by NASA, Ecosun-101 by Ecoprogetti, Sinus-220 by Wavelabs, or SUNLIKE by FutureLED as the most relevant examples) to small areas (those from Newport, Wacom, Innovations in Optics, or FutureLED), and currently, there are still efforts to validate their operation [11]–[13]. The examples most related to the proposal of this paper are analyzed here. LSH-7320 (MiniSol) from Oriel/Newport is an 8.4-kg LED solar simulator ranking Class A, except for a Class B in homogeneity, tunable from 0.1 to 1.1 suns over a  $51 \times 51 \text{ cm}^2$  illumination area located 190–450 mm under its LED printed circuit board (PCB) head, emitting in a 400–1000-nm range. An LSH-7520 LED head and an LSS-7120 driver are the combination inside the VeraSol-2, a Class AAA tunable from 0.1 to 1 sun over a  $51 \times 51$  area at 203-mm distance from the head. It includes 12 LED types that can tune six spectral bands. A universal serial bus (USB) connector allows the control of the emitted spectra, with a fast warm-up time. LumiSun of Innovation Optics is a 2-kg system that can also dim from 0.1 to 1.1 suns and uses distance to control the power received in a  $5 \times 5 \text{ cm}^2$  area. LEDSim by AESCUSOFT includes emission under 400 nm, it can be tuned by software and it uses 20 types of LEDs. Hyperion from Greatcellsolar (former Dyesol) also achieves the AAA Class in a  $23 \times 23 \text{ cm}^2$  area, with the possibility of tuning the spectral emission from 0 to

1 sun, although not in all wavelengths. Summing up, most of the commercial solutions incur some of these drawbacks: they are expensive, or at least too expensive to have more than 1, or they are heavy, or include optics, or are difficult to be tuned, or are above the scope of a small laboratory, or over the need of characterizations of new small prototype devices under research. It could be necessary for a truly low-cost system that integrates all the outcomes that commercial solutions offer in a small scale to easily reproduce.

In this line of work, and more recently, 15 LEDs were used in a student's approach [25] providing a variable output from 0.1 to 1.0 sun using a set of MOSFETs as drivers, triggered by pulsewidth modulation signals, using an Arduino-like microcontroller, but with a low homogeneity (Class C). Wang *et al.* [26] use a numerical algorithm by MATLAB to obtain a theoretical estimation of the number of LEDs needed for achieving the solar spectrum using 14 wavelengths. Xu *et al.* [27] sweep the market to explore 103 kinds of LEDs, obtaining a theoretical 380–780-nm sun simulator by fitting the emissions of 34 of them to a spectrum that approximates to 88.7% of the sun one, and seeking how this fitting reduces when decreasing the number of LED types. In the lower limit of the low cost, Nakajima *et al.* [28] used even a single LED with a cover of a custom phosphor powder to achieve a broadband sun simulator.

At the light of these studies and having also the necessity of testing new small prototypes of solar cells in our lab, we have tried another approach that intends an integration of every above-presented feature that meets with low-cost, reproducibility, and customizability requirements. We proposed the objective of designing and building a low-cost Class AAA solar simulator based only on the LED technology, without using any kind of optics or concentrators, completely software tunable in irradiance and spectrum by using off-the-shelf components, and with the aim of being easily reproducible in any research lab. Consequently, we have designed and built a light, small, and Arduino-controlled LED sun simulator, using an ultralow cost and easy to replicate fabrication procedure by 3-D printing the full structure in PLA plastic. This paper describes the result of this attempt and its calibration.

In the following sections, we will focus on: the design of the prototype, with its simulations, spectral match, and homogeneity estimations (Section II); the development of the device, in hardware and software terms (Section III); and its calibration procedure to determine the AAA Class of the device (Section IV). Section V will compare our proposal with the devices that are found in both the literature and the market. Final conclusions will serve to stress the interest of the system for the solar cells community in order to apply it in their experiments with prototypes.

## II. DESIGN

To achieve the above-mentioned goals, we propose a small solar simulator made only with LED technology, to obtain more durable, reliable, and stable light, besides using a more ecological approach. Fig. 1 shows the geometry principle of

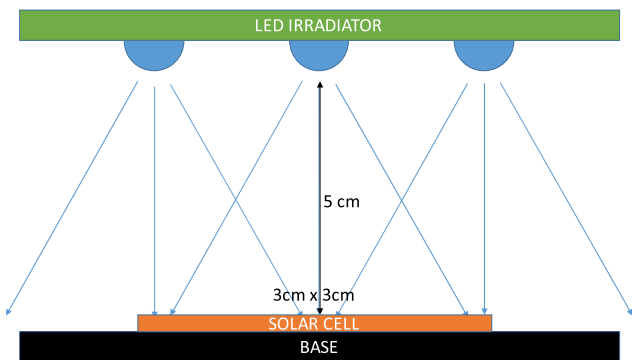


Fig. 1. Schematic design of the solar simulator.

the design: to create a PCB of 5 cm  $\times$  5 cm full of LEDs in such a distribution as to project a sun-like irradiance in a plane surface region parallel to it and 5 cm below, where the prototype solar cells will be placed. We name this plane under the LEDs PCB the sample plane. We will irradiate a square area of 3 cm  $\times$  3 cm, which is over the usual size of the new solar prototyped cells that we characterize (around 1 cm<sup>2</sup>). These dimensions force the size of the LEDs PCB. The design must leave room to place the cell and its contacts in the sample plane because we need it to be irradiated while measuring parameters such as  $I$ - $V$  curves or performing EIS characterization. We use perovskites and organic solar cells, which are active in the visible range and silicon solar cells, which are active in near infrared (NIR). Although all of them could also be degraded by the UV radiation. Thus, all these wavelengths should be used in our simulator.

The proposed design does not include any kind of optics (filters and lenses) because we want to keep the design as cheap as possible. The other goal is exploring the possibility of achieving a solar simulator with enough quality to test solar cells as the commercial sun simulators perform, but maintaining the reproducibility of the manufacturing and a lot of custom functionalities.

We used MATLAB software from MathWorks to design and simulate the system. The first feature to design is the irradiance of each LED projected in the sample plane. Using the values of optically emitted power of each individual selected LED, our MATLAB script must obtain the values of spectral irradiance in each point of the irradiated surface in the sample plane. Then, the script must integrate the spectral irradiance in the whole spectrum to obtain the value of irradiance in mW/cm<sup>2</sup> at each point of the sample plane.

At the first time, we made a selection of commercial LEDs to be used as illuminators in our system. The criteria for the whole set were: high efficiency (high radiance with low current), covering the spectral range from 350 to 1100 nm, and able to be tuned to achieve a solar-like response. The 14 off-the-shelf LED types were selected, each one with an emission centered at different wavelengths. These central wavelengths were spread along the 350–1100-nm range to have the possibility of fine-tuning the total irradiance. The number of 14 different central wavelengths is the result of having the lower number of LED types to accomplish all

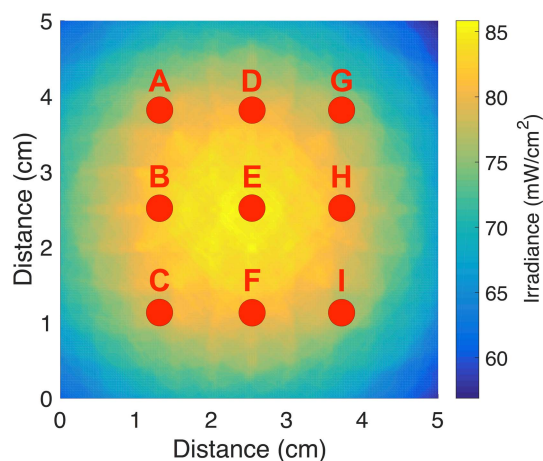


Fig. 2. Simulated irradiance spatial distribution with nine calibration points.

the above criteria. Table I summarizes the selected LEDs and shows that their price is as low to accomplish the low-cost objective for the overall system. The selection was also supported by the ratio between the radiant flux and efficacy, both shown in Table I.

Class AAA solar simulator is defined in the IEC60904-9 standard [1]. The PCB LED area of 5 cm  $\times$  5 cm was divided into 100 squares to place the LEDs on them. In order to achieve this qualification in our system, we performed an iterative simulation process with our MATLAB procedure, varying the number and positions of each type of LED, until we had the correct spatial distribution in the sample plane (Fig. 1) that provided the spectrum as close as possible to AM1.5G with the minimum number of LEDs. The spectral data of the AM1.5G spectrum standard were obtained from the National Renewable Energy Laboratory web page [29].

Fig. 2 shows the irradiance distribution in the whole area 5 cm below the 34 LEDs PCB created a surface. The irradiance reaches and even exceeds the value of 1 sun in the AM1.5G that we were searching for (an integrated value of 81.75 mW/cm<sup>2</sup> in the 300–1100-nm wavelength interval). This area is split into nine points in order to compute the total irradiance at every point marked in Fig. 2 for the step of homogeneity calibration, once we had built the device. This calibration will be explained in the following section. For having a more comfortable figure and to ease the comparison with the literature, the units are given in mW/cm<sup>2</sup>.

The spectral irradiance simulation obtained in the central point of the sample plane is shown in Fig. 3. All the irradiances coming from each LED are computed; taking into account, all the angular effects both in emission—following their datasheets spatial distributions, and reception—applying a cosine correction. This is a shot of the central point ( $E$ -point) of Fig. 2. The back yellow line represents the AM1.5G solar spectrum, and the black line represents the total spectrum of our system. We plot another 14 lines that represent the spectra given by each set of LEDs. Some void intervals (close to 650 and 775 nm) are compensated by increasing the

TABLE I  
CHARACTERISTICS OF THE USED LEDs

Reference	Peak Wavelength (typ.)	Radiant/Luminous Flux (typ.)	Radiant/Luminous Efficacy	Price per unit
VLMU3510-365-130	367 nm	690 mW	345 mW/W	15.36 \$
VLMU3510-385-120	385 nm	780 mW	458.8 mW/W	8.38 \$
L1F3-U400200012000	400 nm	1300 mW	419.4 mW/W	8.50 \$
GD CSSPM1.14	451 nm	690 mW	690 mW/W	1.69 \$
GB DASPA1.13	465 nm	7.5 lm	23 lm/W	0.83 \$
GT CSSPM1.13	521 nm	130 lm	111 lm/W	2.14 \$
GT PSLR31.13	540 nm	170 lm	181 lm/W	0.57 \$
LXML-PX02-0000	567 nm	184 lm	191 lm/W	4.85 \$
GY CSHPM1.23	593 nm	76 lm	99 lm/W	2.14 \$
GA CSSPM1.23	625 nm	100 lm	136 lm/W	1.87 \$
GR PSLR31.13	650 nm	24 lm	26 lm/W	0.64 \$
GF CSSPM1.24	730 nm	317 mW	430 mW/W	3.33 \$
15435385AA350	855 nm	710 mW	323 mW/W	4.08 \$
15435394AA350	945 nm	620 mW	326 mW/W	4.98 \$

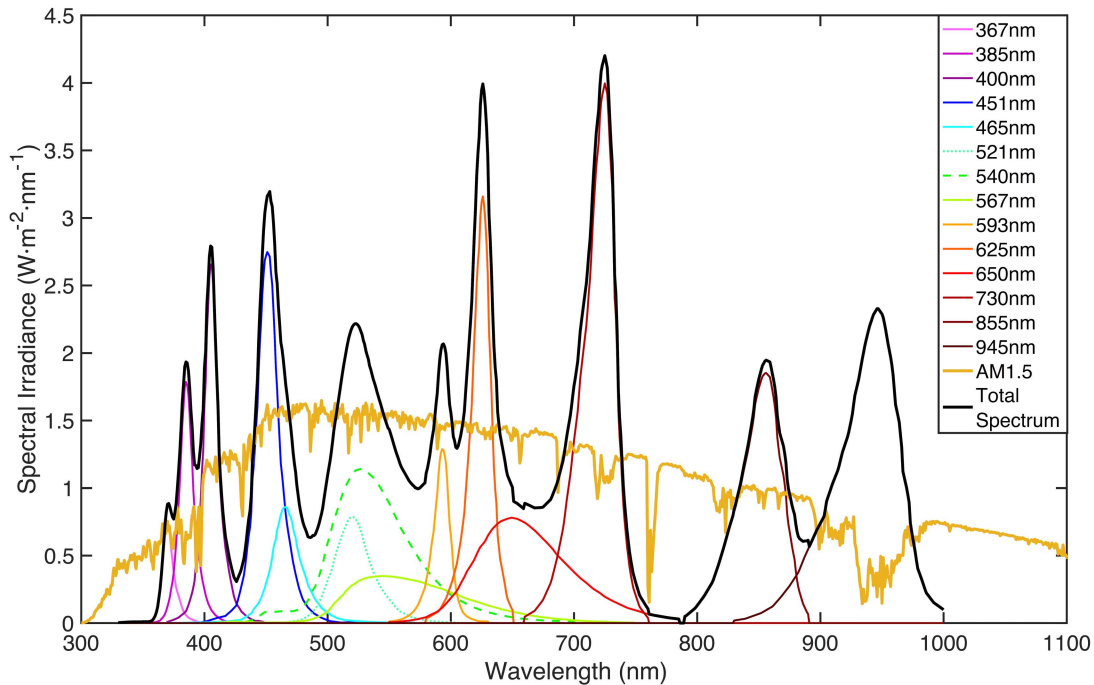


Fig. 3. Simulated spectral irradiance versus AM1.5G spectra.

power of the surrounding LEDs in order to obtain the desired 1-sun irradiance.

Following the above-mentioned IEC60904-9, we have three categories, and our design must accomplish a Class A in every one of them. These three categories are the spectral match, homogeneity, and temporal stability. They will be discussed

hereunder using the data obtained after the simulation of the designed setup.

#### A. Spectral Match

The goal here is to obtain less than  $\pm 25\%$  of deviation against the AM1.5G spectrum integrated along each one of



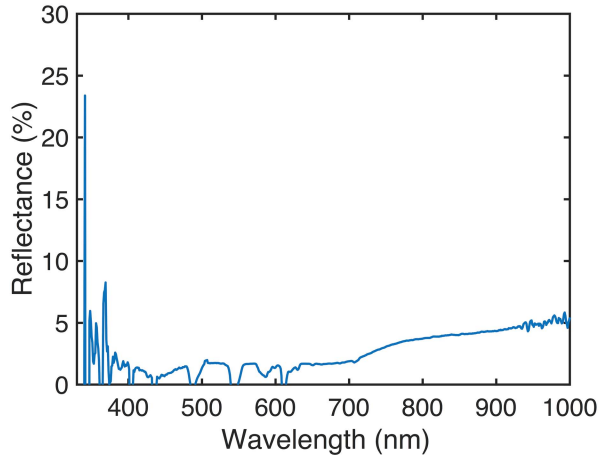


Fig. 4. Averaged reflectance of PLA plastic measured at several points of the structure.

TABLE II  
IRRADIANCE DEVIATION IN THE SIMULATION WITH AM1.5G

Spectral Interval (nm)	Simulated (mW/cm <sup>2</sup> )	AM1.5G (mW/cm <sup>2</sup> )	Deviation (%)
300-400nm	4.47 mW/cm <sup>2</sup>	4.64 mW/cm <sup>2</sup>	-4%
400-500nm	14.23 mW/cm <sup>2</sup>	14.09 mW/cm <sup>2</sup>	1%
500-600nm	15.85 mW/cm <sup>2</sup>	15.25 mW/cm <sup>2</sup>	4%
600-700nm	15.82 mW/cm <sup>2</sup>	14.06 mW/cm <sup>2</sup>	13%
700-800nm	12.56 mW/cm <sup>2</sup>	11.44 mW/cm <sup>2</sup>	10%
800-900nm	9.62 mW/cm <sup>2</sup>	9.54 mW/cm <sup>2</sup>	1%
900-1100nm	12.36 mW/cm <sup>2</sup>	12.15 mW/cm <sup>2</sup>	2%
Total Irradiance	84.91 mW/cm <sup>2</sup>	81.18 mW/cm <sup>2</sup>	5%

the wavelengths intervals specified in the standard: 400–500, 500–600, 600–700, 700–800, 800–900, and 900–1100 nm. These deviations were calculated using the following equation:

$$\text{Deviation}_{(\lambda_1, \lambda_2)} = \left( \frac{\int_{\lambda_1}^{\lambda_2} I_{\text{AM1.5G}}(\lambda) - \int_{\lambda_1}^{\lambda_2} I_{\text{Simulated}}(\lambda)}{\int_{\lambda_1}^{\lambda_2} I_{\text{AM1.5G}}(\lambda)} \right) \cdot 100[\%]. \quad (1)$$

Although the ultraviolet-A zone (300–400 nm) is out of normative, we also tried to achieve a “Class A” in this interval. Table II lists the results of deviation after the theoretical calculations of the currents.

We can see from Table II that we have values of deviation much lower than  $\pm 25\%$ , so according to our design simulations, we achieve a Class A solar simulator.

### B. Homogeneity

Regarding spatial homogeneity, we must reach a value lower than 2% to achieve the Class A threshold. A homogeneous irradiance ensures that the tested device will be equally irradiated in all its surface. Table III lists the results of our design at the nine points that were marked in Fig. 2.

The homogeneity factor is calculated using the following equation:

$$\text{Homogeneity} = \frac{I_{\text{MAX}} - I_{\text{MIN}}}{I_{\text{MAX}} + I_{\text{MIN}}} \cdot 100[\%] \quad (2)$$

TABLE III  
IRRADIANCE VALUES ON THE HOMOGENEITY SIMULATION

Zone	Irradiance
A	77.77 mW/cm <sup>2</sup>
B	80.70 mW/cm <sup>2</sup>
C	75.09 mW/cm <sup>2</sup>
D	82.59 mW/cm <sup>2</sup>
E	84.19 mW/cm <sup>2</sup>
F	80.29 mW/cm <sup>2</sup>
G	78.21 mW/cm <sup>2</sup>
H	81.60 mW/cm <sup>2</sup>
I	76.03 mW/cm <sup>2</sup>

where  $I_{\text{MAX}} = 84.19$  [mW/cm<sup>2</sup>] and  $I_{\text{MIN}} = 75.09$  [mW/cm<sup>2</sup>]. Doing this operation, we obtain a value of 5.71%, which is almost a Class B solar simulator in this 3 cm × 3 cm tested area. However, if we reduce the area to 1 cm × 1 cm around the central point of the sample plane (E), which is a typical dimension for our tested devices, we obtain a 1.77% value. We can see that this factor is below the 2% limit, so, theoretically, we have a Class A solar simulator in terms of homogeneity at this central area of 1 cm<sup>2</sup>.

### C. Temporal Stability

This feature consists of two parts, the long-term instability (LTI) and the short-term instability (STI). To achieve a Class A solar simulator, we must have less than 0.5% of deviation in both of them respect with the standard.

Both the STI and LTI measurements consist of taking a series of measurements of the irradiance during a fixed time and at every certain time interval. Times of STI and LTI are not standard; they depend on the application intended for the sun simulator. In our case, a good reference can be the measurements that will be made while irradiating the samples. Thus, STI time will correspond to the time required to obtain a point of an  $I$ – $V$  curve or an EIS measurement, for example. Similarly, in the LTI measurement, the fixed time will be above the total time that an  $I$ – $V$  curve measurement takes. This parameter cannot be simulated, because it depends on the behavior of the whole system, both electronics and optics, depending on parameters such as the thermal dissipation or the actual amount of power emitted by the LEDs.

All these aspects will be discussed in more detail in the characterization section.

## III. DEVELOPMENT

### A. Hardware

Once our geometrical design was validated by the simulation, we proceeded to design the structure of the device to support the LEDs PCB. We used a CAD software to create a modular structure, in which the geometrical conditions

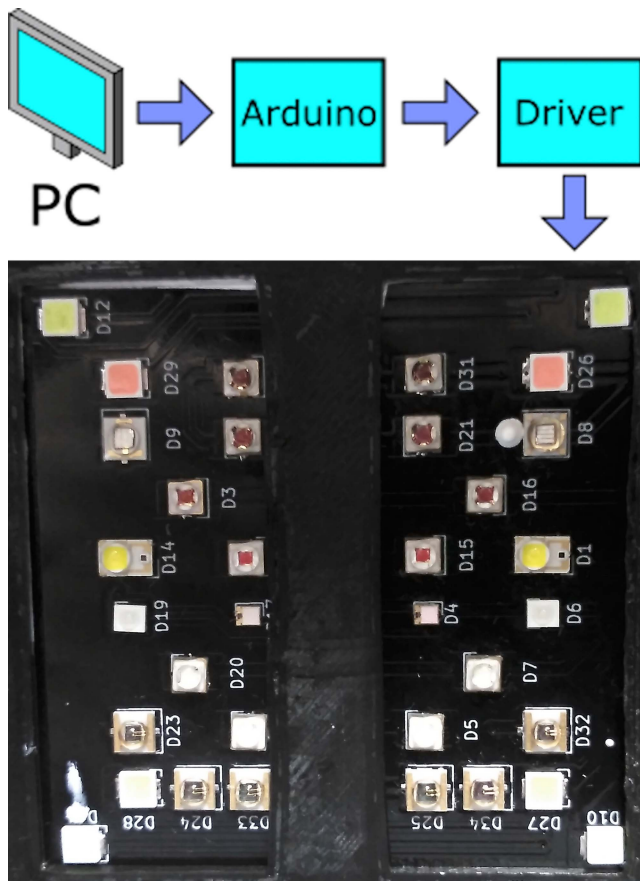


Fig. 5. Schematic of the whole system. A photograph of the LED PCB is shown on the bottom.

described earlier are achieved. Then, we prepared the file to be printed with a 3-D printer loaded with black PLA filament, to avoid reflections of the light, and to reduce stray light in the future measurements. To prove this, we measured the reflectance of this plastic at several random points of the structure, obtaining an averaged reflection value below 3% in the visible range (see Fig. 4).

Both the LED and power PCBs are also designed and implemented by us. Fig. 5 shows a complete diagram of the electronic system. A PC is connected to an Arduino microcontroller that controls the drivers assessing the current through the LEDs. It is a modular design, which can be sliced into three principal parts: the LED PCB, the power electronics PCB, and the control electronics. The CAD design can be seen from Fig. 6(a).

The main problem to undertake in the design of the LEDs PCB is the thermal dissipation of the LEDs. A total of 34 LEDs are driven by a total current of 4.4 A. In those conditions, the electronic design of both the LED PCB and the power electronics is fundamental. We computed requirements such as thermal reliefs, ground and power planes, or the thickness of the tracks. Our solution implements dedicated thermal paths for each LED, in order to remove as much heat as possible, in a four-layer PCB. This design was combined with a heat sink and a simple PC 12-V fan continuously working. In this way, we got a proper cooling system for

the LEDs, to improve their performance and reliability. In the power electronics PCB, we used individual, dedicated drivers for each group of LEDs, and with digital and analog current modulation. Each driver consists of dc/dc power converter, DAC, and proper electronic conditioning in order to act as an adjustable constant current source. This allows us applying a custom constant current of a certain level or a pulsed one at a certain frequency, separately to each group of LEDs, i.e., to each wavelength, depending on the measurement that we want to do. The third board contains the control electronics, which can control every driver of the intermediate PCB. This is a simple Arduino Uno microcontroller, one of the most widely popular and low-cost electronic devices.

Fig. 6(b) shows the manufactured device, with the three modular levels, and all the wiring connections between them. At this point, the device is ready to work.

### B. Software

A National Instruments' LabVIEW application was developed to control the whole system via PC. (Arduino is connected to it via USB interface.) This is a simple, very intuitive, and easy to use application. It is written using Lynx, a LabVIEW add-on to control Arduino. It includes 14 sliders/button areas, each one corresponding to one group of LEDs, i.e., each wavelength of the system. In this way, we can configure how much current flows through every set of LEDs, which implies to control the whole spectrum with 14 separated wavelength intervals. The user can irradiate in a red/green combination or only with ultraviolet, for example.

In Fig. 7(a), we can see the user interface configured to illuminate with 1 sun of power (AM1.5G Spectrum). Each set is accessed separately to obtain the driving current that is needed. Only an end button and a menu to select the serial port where Arduino is connected to the PC are added. Fig. 7(b) shows the device working with all the LEDs lighting at Fig. 7(a) configuration. As shown in Fig. 7(a), some wavelength intervals are still well under their maxima, so higher irradiances could be obtained in them in order to perform specific degradation characterizations at UV, blue, or green light, a very interesting scenario for new generations of perovskite and organic solar cells.

## IV. CALIBRATION PROCEDURE

Once the device was built, we proceeded to characterize it. In this process, we used the next setup built with Ocean Optics instruments, from the source to the computer.

- 1) Cosine corrector CC-3-UV-S, to collect all the light that the device emits and with the ability to measure at specific points of the sample plane. In this way, we will be able to compare the measurements obtained by using this setup with our simulations results of Fig. 2 and Table III, in which we took into account this cosine correction.
- 2) QP400-1-VIS-NIR Optical fiber, to transmit the light from the cosine corrector to the spectrometer. Its transmission is over 95%.

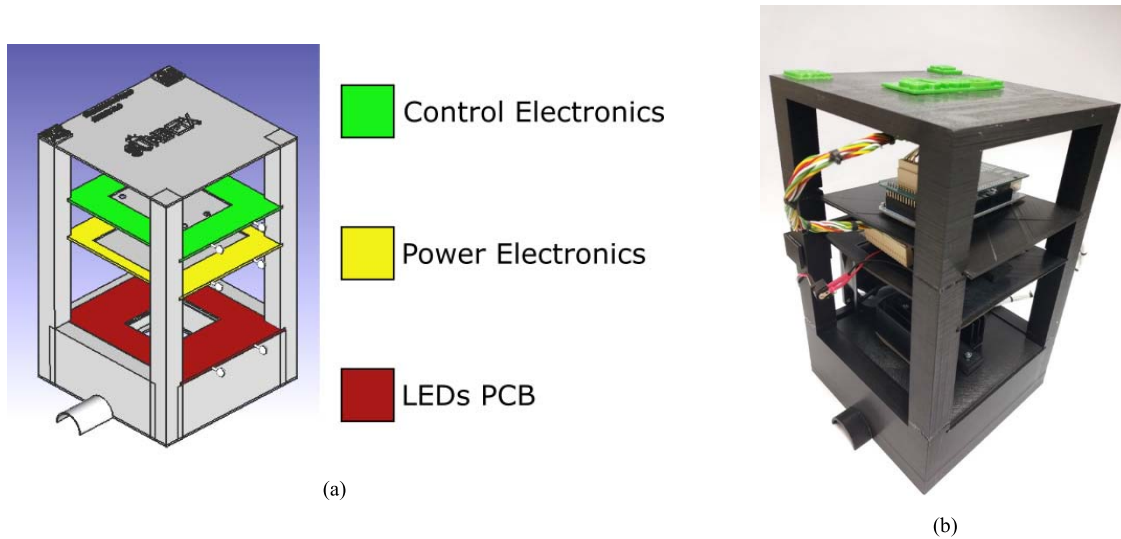
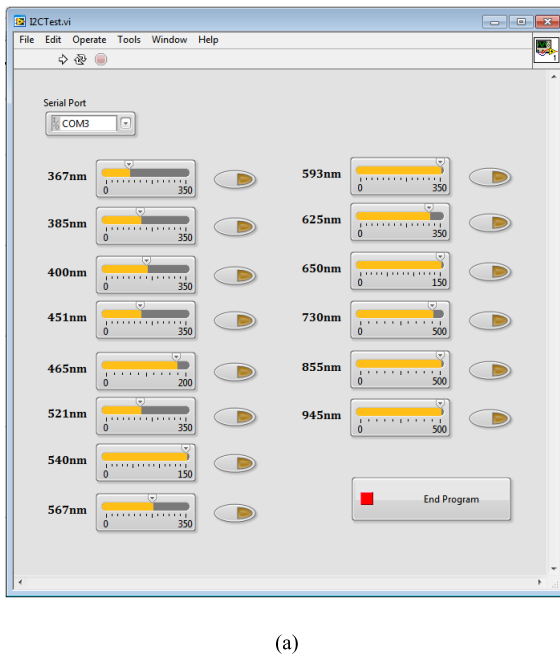


Fig. 6. (a) CAD design of the proposed structure. (b) Fabricated structure with PLA using a 3-D printer.



(a)



(b)

Fig. 7. (a) Device is controlled via computer interface. (b) Adjusting the sliders properly we can achieve the irradiance of 1 sun. Light outcomes from the window where any possible wiring to the cell under test can be fixed.

- 3) USB2000 + Spectrometer, to be able to convert the received light into data, using SpectraSuite software.

We calibrated the whole setup using an HL-3P-CAL lamp to achieve spectral irradiance measurements.

We can see the setup for the characterization process shown in Fig. 8(a). The fiber is placed in a calibration support that we designed and fabricated on 3-D printed PLA too, as the rest of the structure. This calibration base can be easily removed, due to the modularity of the system and the way in which it is built. With this setup, we avoid the usage of another complex measurement system that integrates high quantities of photodiodes to get a complete map of the irradiated area [30].

Using this measurement system, we analyzed the values of each individual set of LED (the same wavelength emission) and the total spectrum of the whole system, in order to compare and to adjust the real measurements with the simulated ones. In Fig. 8(b), we have the experimental measurements in front of the simulated results. We can check the quality of the match between the results using the following equation, which will give us the deviation factor:

$$\text{Deviation}_{(\lambda_1, \lambda_2)} = \left( \frac{\int_{\lambda_1}^{\lambda_2} I_{\text{Simulated}}(\lambda) - \int_{\lambda_1}^{\lambda_2} I_{\text{Measured}}(\lambda)}{\int_{\lambda_1}^{\lambda_2} I_{\text{Simulated}}(\lambda)} \right) \cdot 100[\%]. \quad (3)$$

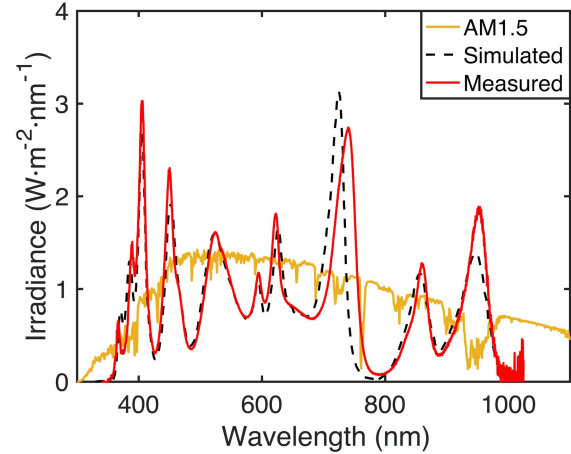
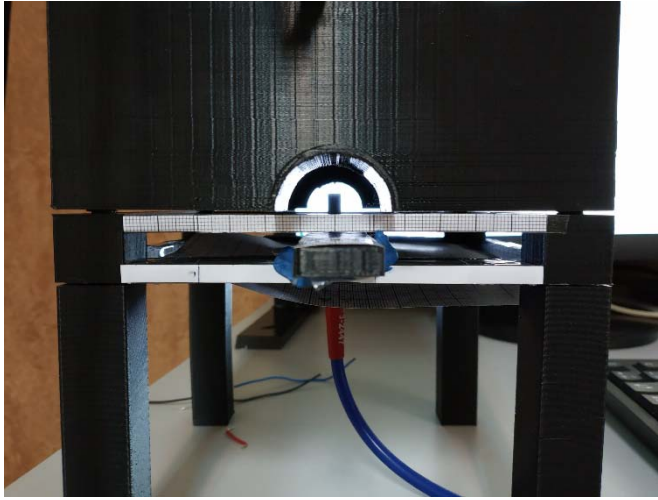


Fig. 8. (a) Calibration and measurement system are used to extract the experimental data. (b) Then, we compare these data with the simulations obtaining a good match.

TABLE IV

DEVIATION BETWEEN EXPERIMENTAL AND SIMULATED RESULTS

Spectral Interval	Simulated	Measured	Deviation
300-400nm	4.47 mW/cm <sup>2</sup>	4.57 mW/cm <sup>2</sup>	2%
400-500nm	14.23 mW/cm <sup>2</sup>	14.69 mW/cm <sup>2</sup>	3%
500-600nm	15.85 mW/cm <sup>2</sup>	15.53 mW/cm <sup>2</sup>	-2%
600-700nm	15.82 mW/cm <sup>2</sup>	15.46 mW/cm <sup>2</sup>	-2%
700-800nm	12.56 mW/cm <sup>2</sup>	13.03 mW/cm <sup>2</sup>	4%
800-900nm	9.62 mW/cm <sup>2</sup>	8.17 mW/cm <sup>2</sup>	-15%
900-1100nm	12.36 mW/cm <sup>2</sup>	11.78 mW/cm <sup>2</sup>	-5%
Total Irradiance	84.91 mW/cm <sup>2</sup>	83.24 mW/cm <sup>2</sup>	-2%

TABLE V

IRRADIANCE DEVIATION BETWEEN MEASUREMENTS AND AM1.5G STANDARD

Spectral Interval	Measured	AM1.5G	Deviation
300-400nm	4.57 mW/cm <sup>2</sup>	4.64 mW/cm <sup>2</sup>	-1%
400-500nm	14.69 mW/cm <sup>2</sup>	14.09 mW/cm <sup>2</sup>	4%
500-600nm	15.53 mW/cm <sup>2</sup>	15.25 mW/cm <sup>2</sup>	2%
600-700nm	15.46 mW/cm <sup>2</sup>	14.06 mW/cm <sup>2</sup>	10%
700-800nm	13.03 mW/cm <sup>2</sup>	11.44 mW/cm <sup>2</sup>	14%
800-900nm	8.17 mW/cm <sup>2</sup>	9.54 mW/cm <sup>2</sup>	-14%
900-1100nm	11.78 mW/cm <sup>2</sup>	12.15 mW/cm <sup>2</sup>	-3%
Total Irradiance	83.24 mW/cm <sup>2</sup>	81.18 mW/cm <sup>2</sup>	3%

Table IV lists the deviation values in the spectral intervals of interest. Seeing these results, we can justify that we have fairly a good fit between the measured spectrum and the one expected from the simulations (less of 5% deviation in all spectral ranges except 800–900 nm). The  $-15\%$  of deviation in 800–900 nm is due to a lack of power in the LEDs that belong to this range, because its corresponding driver cannot reach the required and projected 500 mA of bias current, due to the components' tolerances in the conditioning circuit. This lack of power can be corrected by changing this specific driver. Nevertheless, in the current system, a compensation is performed just by tuning the emissions from the rest of the intervals. Another fact that must be taken into account is the red shift in the set of 730-nm LEDs [Fig. 8(b)]. This displacement is into the tolerance range of the LED device manufacturer datasheet, so the shift is a fabrication issue, and not a design one.

Once we checked that the simulations fit the measurements, we evaluated the Class of our device in the above three referenced terms.

#### A. Spectral Match

We measured the total irradiance spectrum given by our device in point *E* of Fig. 2 when the driver is set at AM1.5G mode and sliced it into different spectral ranges required by the normative. Using the following equation, we evaluate the deviation percentages of our device (Table V):

$$\text{Deviation}_{(\lambda_1, \lambda_2)} = \left( \frac{\int_{\lambda_1}^{\lambda_2} I_{\text{AM1.5G}}(\lambda) - \int_{\lambda_1}^{\lambda_2} I_{\text{Measured}}(\lambda)}{\int_{\lambda_1}^{\lambda_2} I_{\text{AM1.5G}}(\lambda)} \right) \cdot 100[\%]. \quad (4)$$

We can see from Table V that all deviation values are under the  $\pm 25\%$  Class A threshold, so we can conclude that, in terms of the spectral match, our device behaves as a Class A.

#### B. Homogeneity

To evaluate the homogeneity, we measured the same nine points that we evaluated in the simulation (Fig. 2), while the driver is set to the calibrated AM1.5G. The obtained results are shown in Table VI.



TABLE VI  
IRRADIANCE VALUES ON THE HOMOGENEITY MEASUREMENT

Zone	Irradiance
A	83.50 mW/cm <sup>2</sup>
B	83.89 mW/cm <sup>2</sup>
C	75.85 mW/cm <sup>2</sup>
D	80.94 mW/cm <sup>2</sup>
E	84.49 mW/cm <sup>2</sup>
F	82.01 mW/cm <sup>2</sup>
G	77.33 mW/cm <sup>2</sup>
H	80.22 mW/cm <sup>2</sup>
I	76.14 mW/cm <sup>2</sup>

With the results of Table VI and using (2), we calculate the value of the homogeneity factor, obtaining 5.38%, which is a better value than the simulated one (5.71%). Using these results, we can conclude that in this area (3.5 cm × 3.5 cm), we have almost a Class B. If we restrict the area to 1 cm × 1 cm around the central point of the sample plane, we obtain a Class A solar simulator regarding the homogeneity (1.77% of deviation).

### C. Temporal Stability

In this section, we must analyze the STI and LTI, respectively, that cannot be simulated. Two experiments were prepared.

- 1) In the first one, we made five rounds of measurements, each one of 1 s of duration, taking a spectrum every 100 ms. This experiment evaluates the STI.
- 2) In the second one, we made the same five rounds of measurements, but this time we acquired a spectrum every 10 s for 300 s, around the time needed to have an  $I$ - $V$  or an EIS measurement. We took measurements from the moment, in which the LEDs are switched ON. This experiment evaluates the LTI

$$\text{STI or LTI} = \frac{I_{\text{MAX}} - I_{\text{MIN}}}{I_{\text{MAX}} + I_{\text{MIN}}} \cdot 100[\%]. \quad (5)$$

Applying (5), we calculated the STI and LTI percentage factors that are shown in Table VII.

In order to obtain a Class A device, STI and LTI deviation values must stay below 0.5%. Table VII lists that our device is Class A in terms of STI without warm-up time (0.3284%), and Class A in terms of LTI, if we consider a warm-up time of 60 s (0.4582%), by removing the first six measurements of our LTI sets in (5). Moreover, the refrigeration system (heat sink with fan) is able to keep the system on 40 °C under full-operation conditions (1 sun). No temperature deviations have been detected. This guarantees a constant emission of the LEDs, avoiding their thermal drifts.

### D. Power Consumption and Performance of the Drivers

In AM1.5G mode, the whole system drains 1.73 A of current, fed with 12 V, which implies a power consumption

TABLE VII  
STI AND LTI EXPERIMENTAL FACTORS

Round	STI	LTI	LTI
	(No warm-up)	(No warm-up)	(60 s warm-up)
1	0.38 %	0.8512%	0.4511%
2	0.4473 %	1.2338%	0.4386%
3	0.3544 %	1.2471%	0.4516%
4	0.3086 %	1.3847%	0.4958%
5	0.1523 %	1.3166%	0.4541%
Average	0.3284 %	1.2067%	0.4582%

of 20.76 W. We analyzed the power used by LEDs, in order to have an approximate overall efficiency of the system. This gave us a value of around 90%. Therefore, in terms of drivers, we can say that they are efficient and stable, because they are based on a feedback loop which is constantly controlling the current flowing through every LED set. In that way, we can avoid power fluctuations due to the thermal and current drifts, achieving such good STI and LTI as the ones obtained above.

We have also performed a measurement of the electronic drivers' yield, and its dependence on the current driving the LEDs. It is a very important feature for a sun simulator device, as it intends to produce the maximum light intensity with the minimum power losses in the electronics that drive the LEDs. Table VIII lists the ratio between the power consumed by the LEDs and the power that the whole system is using at the same time. That will give the efficiency of the LED driver for each one of the examples. The experiment was made measuring the LEDs voltage drop and the current crossing them, and taking three sets of LEDs (grouped by their wavelength) as an example. Two results can be obtained: on the one hand, the driving efficiency is always higher than 85%; on the other hand, there is also a small decay of it when the current is increased, less than 3% when the current is tripled.

### E. Validation: Comparison With a Conventional Simulator Using a Standard Solar Cell

In order to check the validity of our system, we used the 91 150-V calibrated silicon solar cell system by Newport. It was calibrated by Newport using its classic Sol3A commercial solar simulator, giving a response in units of suns. When irradiating this cell with SunBox configured to 1 sun as calculated above, it provided a value of 1.12 suns, when after a minute of stabilization went down to 1.04 suns approximately.

This value justifies that SunBox is at the same operational level and generates the same response in a solar cell as the commercial solar simulators.

## V. DISCUSSION OF RESULTS

Compared with the other similar systems in the literature analyzed in Section I, our SunBox includes the most relevant low-cost features and advantages of LED-based solar simulators while maintaining the Class AAA performance. Some systems are hybrid (LED and halogen) to allow an emission in

TABLE VIII  
ELECTRONIC DRIVER YIELD

Wavelength (nm)	Bias current (mA)	Input Power (W)	Output Power (W)	Efficiency (%)
540	50	1.27	1.17	92.13
	100	2.69	2.41	89.59
	150	4.24	3.79	89.39
650	50	1.25	1.15	92.00
	100	2.65	2.39	90.19
	150	4.13	3.72	90.07
567	120	0.74	0.65	87.84
	240	1.54	1.32	85.71
	350	2.15	1.84	85.58

the whole spectral range, even using some LED reinforcement in the halogen emission due to temperature constraints, like those in [22], [18], or [31], but our proposal is made only by LEDs, and it reaches Class A, overcoming the result of those systems. It is more related to small systems with a low number of LEDs, but with a significantly lower number than those in [17] or [20]. It does not use any reflector or optics to achieve the AAA Class in contrast with [19] or [21], while ranges a wider wavelength interval than the 400–750 nm in [23]. It improves other low-cost attempts using off-the-shelf components and Arduino microcontroller, reaching AAA Class in contrast with [25] or [28], and using a lower number of LEDs than [27], reaching the theoretical value obtained in [26].

When coming to establishing a comparison with the commercial LED solar devices available in the market, all of them at least with a spectral Class A, we now explore the outcomes of the SunBox presented proposal. SunBox is significantly lighter than most of them, including the 8.4 kg of the simplest LSH-7320 of Newport or the 2-kg LumiSun of Innovation Optics. The latter one controls the emission from 0.1 to 1.1 suns. SunBox can dim each part of the spectrum to achieve these values spectrally less than 0.5-kg system. VeraSol from Oriel/Newport includes at least 12 LED types to get 76 mW/cm<sup>2</sup> in the 400–1100-nm spectral range, an irradiance that overcomes a 10% by SunBox. Six spectral bands can be tuned in VeraSol, but SunBox can be tuned in each one of the 14 LEDs group emissions. AESCUSOFT's LEDSim operation is quite similar to our proposal both in terms of its emission tunability via software and its illumination ranging under 400 nm, as well as linear current regulation for LEDs drivers. However, it uses more than 20 types of LEDs in a long-size arrangement, while we use only 14 in a 5 cm × 5 cm plate. The closest commercial sun simulator to SunBox is maybe Hyperion III by Greatcell Solar, although it uses four LED types more than this work.

On the other hand, none of these devices mention the microcontroller that is used to control them. But in our proposal, we use a simple Arduino Nano microcontroller, an extended off-the-shelf low-cost component that is sufficient to support

the needed program to run. This fact, added to the simple 3-D printing and the low-cost LED and driver PCBs created, results in a system that could be replicated to the number needed in any research lab devoted to the characterization of small solar cells, as it was our objective at the beginning of the design.

## VI. CONCLUSION

We have designed, developed, and calibrated a low-cost LED simulator intended to be used for characterizing small experimental solar cells by using a spectral selective emission. All the used components are off-the-shelf, controlled by simple LED drivers and electronics, and with an Arduino microprocessor as the core of the control.

The system that we have developed goes a step further on the current commercial sun simulators, as it intends to fill a gap: the one that small research groups as ours find when trying to use a small sun simulator for small experimental devices and to tune it for different spectral emissions, with the possibility of even using several simulators for different simultaneous experiments. The proposed sun simulator tailors its emission by controlling the current driving each LEDs group. This allows the control of the emission in different spectral bands. Our proposal uses less LEDs than commercial solutions, both in types and in number, reaching an emission close to 1 sun. Class AAA is achieved in a 1 cm<sup>2</sup> central area, but the irradiance is stable and homogeneous enough to perform characterizations in cells of a wider area, up to 25 cm<sup>2</sup>. The system is 3-D printed in ABS plastic and can be reproduced easily. The validity of the system was checked using the 91150-V calibrated silicon solar cell system by Newport.

Further research will improve the emission in some wavelengths by changing some electronic drivers that have revealed to give lower currents than expected, a fact that has led us to tune the power emitted in the intervals around them to compensate their lower emission. By this change, an even finer tuning of the spectral emission will be achieved to get a perfect match with the AM1.5G spectrum.

## REFERENCES

- [1] N. Taylor, "Equipment and basis of power measurements," in *Guidelines for PV Power Measurement in Industry*, 1st ed. Luxembourg: Office for Official Publications of the European Union, 2010, ch. 3, pp. 23–30.
- [2] V. Esen, S. Sağlam, and B. Oral, "Light sources of solar simulators for photovoltaic devices: A review," *Renew. Sustain. Energy Rev.*, vol. 77, pp. 1240–1250, Sep. 2017.
- [3] M. Pravettoni, R. Galleano, E. D. Dunlop, and R. P. Kenny, "Characterization of a pulsed solar simulator for concentrator photovoltaic cell calibration," *Meas. Sci. Technol.*, vol. 21, no. 11, Sep. 2010, Art. no. 115901.
- [4] R. Gill, E. Bush, P. Haueter, and P. Loutzenhisser, "Characterization of a 6 kW high-flux solar simulator with an array of xenon arc lamps capable of concentrations of nearly 5000 suns," *Rev. Sci. Instrum.*, vol. 86, Dec. 2015, Art. no. 125107.
- [5] N. Thomas *et al.*, "A wide-beam continuous solar simulator for simulating the solar flux at the orbit of mercury," *Meas. Sci. Technol.*, vol. 22, May 2011, Art. no. 065903.
- [6] R. W. Mossa, G. S. F. Shire, P. C. Eames, P. Henshall, T. Hyde, and F. Arya, "Design and commissioning of a virtual image solar simulator for testing thermal collectors," *Solar Energy*, vol. 159, pp. 234–242, Jan. 2018.
- [7] R. Galleano, I. Kröger, F. Plag, S. Winter, and H. Müllejjans, "Traceable spectral irradiance measurements in photovoltaics: Results of the PTB and JRC spectroradiometer comparison using different light sources," *Measurement*, vol. 124, pp. 549–559, Aug. 2018.
- [8] D. Kolberg, F. Schubert, N. Lontke, A. Zwigart, and D. M. Spinner, "Development of tunable close match LED solar simulator with extended spectral range to UV and IR," *Energy Procedia*, vol. 8, pp. 100–105, Apr. 2011.
- [9] G. Leary, G. Switzer, G. Kuntz, and T. Kaiser, "Comparison of Xenon lamp-based and LED-based solar simulators," in *Proc. IEEE 43rd Photovoltaic Spec. Conf.*, Jun. 2016, pp. 3062–3067.
- [10] J. Shao *et al.*, "The investigation on hydrogenation platform for silicon solar cells based on high intensity infrared LEDs," *J. Renew. Sustain. Energy*, vol. 10, Jan. 2018, Art. no. 013507.
- [11] L. Cojocaru *et al.*, "Determination of unique power conversion efficiency of solar cell showing hysteresis in the I-V curve under various light intensities," *Sci. Rep.*, vol. 7, Sep. 2017, Art. no. 11790.
- [12] L. N. Inasaridze *et al.*, "Light-induced generation of free radicals by fullerene derivatives: An important degradation pathway in organic photovoltaics?," *J. Mater. Chem. A*, vol. 5, no. 17, pp. 8044–8050, 2017.
- [13] M. D. Heinemann *et al.*, "Evaluation of recombination losses in thin film solar cells using an LED sun simulator—The effect of RbF post-deposition on CIGS solar cells," *EPJ Photovolt.*, vol. 9, p. 9, Sep. 2018.
- [14] T. Luka, S. Eiternick, and M. Turek, "Rapid testing of external quantum efficiency using LED solar simulators," *Energy Procedia*, vol. 77, pp. 113–118, Aug. 2015.
- [15] S. A. Hosseini, A. M. Kermani, and A. Arabhosseini, "Experimental study of the dew formation effect on the performance of photovoltaic modules," *Renew. Energy*, vol. 130, pp. 352–359, Jan. 2019.
- [16] P. Vincent *et al.*, "Indoor-type photovoltaics with organic solar cells through optimal design," *Dyes Pigments*, vol. 159, pp. 306–313, Dec. 2018.
- [17] F. C. Krebs, K. O. Sylvester-Hvid, and M. Jørgensen, "A self-calibrating led-based solar test platform," *Prog. Photovolt.*, vol. 19, no. 1, pp. 97–112, 2011.
- [18] G. Grandi, A. Ienina, and M. Bardhi, "Effective low-cost hybrid LED-halogen solar simulator," *IEEE Trans. Ind. Appl.*, vol. 50, no. 5, pp. 3055–3064, Sep./Oct. 2014.
- [19] M. Stuckelberger *et al.*, "Class AAA LED-based solar simulator for steady-state measurements and light soaking," *IEEE J. Photovolt.*, vol. 4, no. 5, pp. 1282–1287, Sep. 2014.
- [20] F. Plyta, "Optical design of a fully LED-based solar simulator," Ph.D. dissertation, Loughborough Univ., Loughborough, U.K., 2015.
- [21] A. Novičkovas, A. Baguckis, A. Mekys, and V. Tamošiūnas, "Compact light-emitting diode-based AAA class solar simulator: Design and application peculiarities," *IEEE J. Photovolt.*, vol. 5, no. 4, pp. 1137–1142, Jul. 2015.
- [22] F. Schubert and D. Spinner, "Solar simulator spectrum and measurement uncertainties," *Energy Procedia*, vol. 92, pp. 205–210, Aug. 2016.
- [23] N. Riedel, A. A. S. Lancia, S. Thorsteinsson, and P. B. Poulsen, "Validation of the spectral mismatch correction factor using an LED-based solar simulator," presented at the 5th Int. Workshop LED Solar Appl., Kongens Lyngby, Denmark, 2017.
- [24] M. L. D. Scherff, J. Nutter, P. Fuss-Kailuweit, J. Suthues, and T. Brammer, "Spectral mismatch and solar simulator quality factor in advanced LED solar simulators," *Jpn. J. Appl. Phys.*, vol. 56, Jul. 2017, Art. no. 08MB24.
- [25] Y. Pei, "Design of an LED-based solar simulator," M.S. thesis, Murdoch Univ., Perth, WA, Australia, 2017.
- [26] J. Wang, S. Su, G. Zhang, and J. Zhang, "A synthetic method of solar spectrum based on LED," *Proc. SPIE*, vol. 10461, Oct. 2017, Art. no. 104610I.
- [27] G.-Q. Xu, J.-H. Zhang, G.-Y. Cao, M.-S. Xing, D.-S. Li, and J.-J. Yu, "Solar spectrum matching using monochromatic LEDs," *Lighting Res. Technol.*, vol. 49, no. 4, pp. 497–507, 2017.
- [28] T. Nakajima, K. Shinoda, and T. Tsuchiya, "Single-LED solar simulator for amorphous Si and dye-sensitized solar cells," *RSC Adv.*, vol. 4, no. 37, pp. 19150–19171, 2014.
- [29] *National Renewable Energy Laboratory*. Accessed: Aug. 27, 2018. [Online]. Available: <https://rredc.nrel.gov/solar/spectra/am1.5/>
- [30] K. K. Chong and T. K. Yew, "Novel optical scanner using photodiodes array for two-dimensional measurement of light flux distribution," *IEEE Trans. Instrum. Meas.*, vol. 60, no. 8, pp. 2918–2925, Aug. 2011.
- [31] K. A. Kim, N. Dostart, J. Huynh, and P. T. Krein, "Low-cost solar simulator design for multi-junction solar cells in space applications," Presented at the IEEE Power Energy Conf. (PECI), Champaign, IL, USA, Feb./Mar. 2014.



**Eduardo López-Fraguas** was born in Madrid, Spain, in 1994. He received the B.S. degree in industrial electronics and automatics engineering and the M.S. degree in advanced electronic systems engineering from the University Carlos III of Madrid (UC3M), Leganés, Spain, in 2016 and 2017, respectively, where he is currently pursuing the Ph.D. degree in electric, electronic, and automatic engineering.

He is currently a Research Assistant with the Displays and Photonics Applications Group, UC3M.



**José M. Sánchez-Pena** (SM'02) was born in Lugo, Spain, in 1962. He received the M.S. and Ph.D. degrees in telecommunication engineering from the Polytechnic University of Madrid, Madrid, Spain, in 1988 and 1993, respectively.

In 1993, he joined Exeter University, Exeter, U.K., as a Visiting Researcher, where he was involved in modeling of electro-optical devices. In 1995, he joined the Carlos III University of Madrid, Leganés, Spain, where he is currently a Professor and the Head of the Displays and Photonics Applications

Group, Electronic Technology Department. He was the Team Leader of the prototype "Reading Glasses," which was selected by *TIME Magazine* (USA) as one of "The Best Inventions of the Year 2007" in the Entertainment Section. He is currently the Deputy Director and the Head of the Research of the Spanish Centre of Subtitling and Audio-Description, Royal Board on Disability. He has co-authored over 100 papers in JCR journals. His current research interests include electro-optical devices, optical sensors, and optoelectronic instrumentation for assistive technology applications.



**Ricardo Vergaz** received the M.Sc. degree in physics and electronics engineering and the Ph.D. degree in science (Physics) from the University of Valladolid, Valladolid, Spain, in 2001.

He was a Supervisor of two Ph.D. dissertations and a Co-Supervisor of another two. Since 2001, he has been with the Universidad Carlos III de Madrid, Leganés, Spain, where he is currently an Associate Professor with the Displays and Photonics Applications Group, Department of Tecnología Electrónica. He has co-authored over 40 JCR-indexed

publications and 60 communications in international conferences. His current research interests include electro-optical materials and devices characterization, technical aids for visual impairment, and design of novel nanometric devices using scattering directionality.